Orientation of Adsorbed Dyes in the Interlayer Space of Clays. 1. Anisotropy of Rhodamine 6G in Laponite Films by Vis-Absorption with Polarized Light

V. Martínez Martínez, F. López Arbeloa,* J. Bañuelos Prieto, and I. López Arbeloa

Departamento de Química Física, Universidad del País Vasco-EHU. Apartado 644, 48080-Bilbao, Spain

Received April 5, 2005. Revised Manuscript Received May 26, 2005

X-ray diffraction and Vis-absorption spectroscopy with linearly polarized light are used to determine the orientation of rhodamine 6G (R6G) dye in the interlayer space of supported films of Laponite B (Lap) clay with different dye loadings. XRD profiles suggest that the d_{001} interlayer space increases with the relative amount of dye in the clay surface, probably due to a more perpendicular disposition of the adsorbed molecules with respect to the clay layers in high dye content films. This orientation reduces the covering area per adsorbed molecule, providing a more compact and packed arrangement of the dye molecules. This is confirmed by linearly polarized absorption spectra, from which the orientation angle of the adsorbed molecules with respect to the clay layer can be evaluated. Indeed, R6G/Lap supported films present an anisotropy effect and, depending on the dye loadings, different evolutions of the dichroic ratio with the twisted δ angle between the normal to the film and the incident beam are observed. For very diluted R6G/Lap films, the R6G monomers adopt an inclined disposition of around 62° with respect to the film normal. Increasing the loadings, dimer, and higher-order aggregates of R6G can be disposed in two preferential orientations: an inclined angle of around 60°, common in all loading samples, favors long-displaced coplanar aggregates, characterized by an absorption J-band, and a second more perpendicular disposition of the monomer units as the dye content is increased leading to short-displaced coplanar aggregates, identified by an absorption H-band.

Introduction

In the development of electronic and photonic devices, important technological efforts are focused on elaborating hybrid host−guest materials, in which different complementary properties of organic compounds (i.e., structural flexibility and electronic properties) and inorganic matrixes (i.e., thermal and mechanical stability) are combined. Many chemical components in optic sensors, tunable solid-state lasers, optical switches, dichroic filters, double-frequency crystals, solar cells, optical storage devices, antenna systems, and light-emitting diodes are based on hybrid host−guest systems.[1−14] Moreover, depending on the structure of the inorganic matrix, host materials with 1-, 2-, or 3-dimensional arrays in the nanoscale space domain are now available.

In this sense, layered structure materials, such as smectite-type clays, are important matrixes to design highly ordered bidimensional films.[1,5] Besides, clay films possess a high optical transparency (required for most of the optoelectronic applications) and a high capacity to adsorb cationic dyes.[15] Clay materials are suitable systems with interesting applications in modified electrodes, sensors, photochromic devices, and nonlinear optics.[16−21] The immobilization of guest molecules with a preferential arrangement in ordered clay matrixes can result in a desired alignment of photofunctional molecules in a macro-scale domain.[22−31]

* Corresponding author. Phone: +34 94 601 59 71. Fax: +34 94 601 35 00. E-mail: fernando.lopezarbeloa@ehu.es.

(1) Schulz-Ekloff, G.; Wöhrle, D.; van Duffel, B.; Schoonheydt, R. A. *Microporous Mesoporous Mater.* **2002**, *51*, 91−138.
(2) Calzaferri, G.; Huber, S.; Maas, H.; Minkowski, C. *Angew. Int. Ed.* **2002**, *42*, 3732−3758.
(3) Mitzi, D. B. *Chem. Mater.* **2001**, *13*, 3283−3298.
(4) Ramamurthy, V.; Eaton, D. F. *Chem. Mater.* **1994**, *6*, 1128−1136.
(5) Ogawa, M.; Kuroda, K. *Chem. Rev.* **1995**, *95*, 399−438.
(6) Nalwa, H. S., Ed. *Handbook of Advanced Electronic and Photonic Materials and Devices*; Academic Press: San Diego, CA, 2001.
(7) Thomas, J. K. *Chem. Rev.* **1993**, *93*, 301−320.
(8) Schrader, S.; Penzkofer, A.; Holzer, W.; Velagapudi, R.; Grimm, B. *J. Lumin.* **2004**, *110*, 300−308.
(9) Fan, Q.; McQuillin, B.; Bradley, D. D. C.; Whitelegg, S.; Seddon, A. B. *Chem. Phys. Lett.* **2001**, *347*, 325−330.
(10) Arena, A.; Patané, S.; Saitta, G.; Rizzo, G.; Galvagno, S.; Neri, G. *J. Non-Cryst. Solids* **2003**, *331*, 263−268.
(11) Miled, O. B.; Grosso, D.; Sanchez, C.; Livage, J. *J. Phys. Chem. Solids* **2004**, *65*, 1751−1755.
(12) Wu, P.; Bhamidipati, M.; Coles, M.; Rao, D. V. G. L. N. *Chem. Phys. Lett.* **2004**, *400*, 506−510.
(13) Liao, J.-Y.; Ho, K.-C. *Sol. Energy Mater. Sol. Cells* **2005**, *86*, 229−241.
(14) Geng, Y.; Gu, D.; Gan, F. *Opt. Mater.* **2004**, *27*, 193−197.
(15) Yariv, S. In *Modern Approaches to Wettability*: *Theory and Applications*; Malcon, E., Schrader, E., Loed, G., Ed.; Plenum Press: New York, 1992.
(16) Umemura, Y.; Yamagishi, A.; Schoonheydt, R. A.; Persons, A.; De Schryver, F. *J. Am. Chem. Soc.* **2002**, *124*, 992−997.
(17) Van Duffel, B.; Schoonheydt, R. A.; Grim, C. P. M.; De Schryver, F. C. *Langmuir* **1999**, *15*, 7520−7529.
(18) Van Duffel, B.; Verbiest, T.; Elshocht, V.; Persoons, A.; De Schryver, F. C.; Schoonheydt, R. A. *Langmuir* **2001**, *17*, 1243−1249.
(19) Lee, H. C.; Lee, T. W.; Lim, Y. T.; Park, O. O. *Appl. Clay Sci.* **2002**, *21*, 287−293.
(20) Pecorari, M.; Bianco, P. *Electroanalysis* **1998**, *10*, 181−186.
(21) AeBaron, P. C.; Wang, Z.; Pinavaia, T. J. *Appl. Clay Sci.* **1999**, *15*, 11−29
(22) Schoonheydt, R. A. *Clays Clay Miner.* **2002**, *50*, 411−420.
(23) Fujita, T.; Iyi, N., Kosugi, T.; Ando, A.; Deguchi, T.; Sota, T. *Clays Clay Miner.* **1997**, *45*, 77−84.
(24) Iyi, N.; Sasai, R.; Fujita, T.; Deguchi, T.; Sota, T.; López Arbeloa, F.; Kitamura, K. *Appl. Clay. Sci.* **2002**, *22*, 125−126.
(25) Bujdak, J.; Iyi, N.; Kaneko, Y.; Czímerová, A.; Sasai, R. *Phys. Chem. Chem. Phys.* **2003**, *5*, 4680−4685.
(26) Sonobe, K.; Kikuta, K.; Takagi, K. *Chem. Mater.* **1999**, *11*, 1089−1093.

10.1021/cm050728k CCC: $30.25
Published on Web 07/02/2005

Scheme 1. Absorption Characteristics for Dimers with Different Geometries and Orientations with Respect to the Clay-Layer Plane Proposed by the Exciton Theory[39,40]

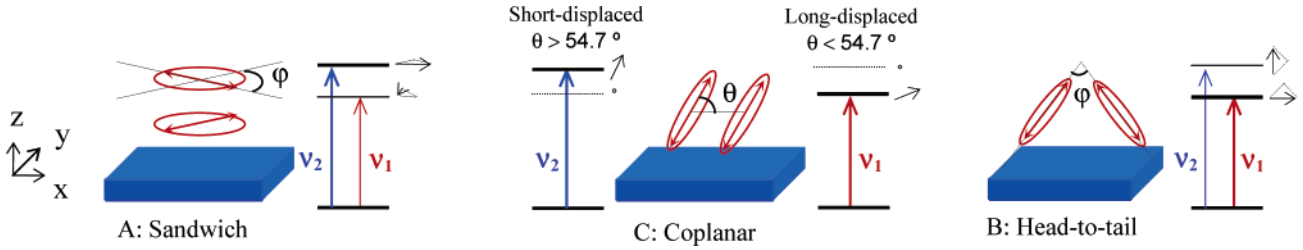

In the present paper, the anisotropy behavior of rhodamine 6G (R6G, see **1**) intercalated in ordered Laponite (Lap) clay

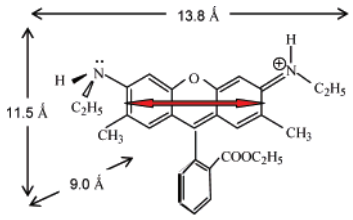

1

layers is studied by Vis-absorption with linearly polarized light. Macroscopic arrangements of clay layers are obtained by the elaboration of supported thin films by the spin-coating technique.[32] The preferential orientation of the dye is checked by recording the response of the absorption spectrum of the dye to the horizontally and vertically polarized incident light by changing the orientation angle between the normal to the film and the incident light. This study is performed in films with different dye loadings, where R6G molecules can be adsorbed on Lap films as monomers, dimers, and higher-order aggregates.[33,34]

The polarized light absorption technique is based on the interaction between the transition moment vector ($\vec{\mathbf{M}}$) of the absorbing molecule with the electric field vector ($\vec{\mathbf{E}}$) of the incident light oscillating in the polarization plane.[35−38] The absorption intensity will depend on the ψ angle between both vectors. Indeed, the dichroic ratio, defined as the relation between the absorbance of the sample for two perpendicularly polarized lights to each other (i.e., *X*- and *Y*-axes) and perpendicular to the incident light (*Z*-axis in this case), $D_{X,Y} = A_X/A_Y$ is related to the angle between the normal to the clay layer and the incident beam (δ) by means of

$$D_{X,Y} = \frac{A_X}{A_Y} = 1 + \frac{2 - 3\sin^2\psi}{\sin^2\psi}\sin^2\delta \qquad (1)$$

For more details, see Scheme 2 in the Experimental Section. The mathematical procedure is developed in an Appendix included as Supporting Information. Consequently, absorption spectra with polarized light can provide information about the relative orientation of the molecules if the polarized plane is known (controlled by the orientation of the polarizer).

For xanthene-type dyes such as R6G, the transition moment lies along the long-molecular axis,[38] and the anisotropy of the absorption light directly provides the orientation of the xanthene plane if the dye is adsorbed on the clay films as monomer units (e.g., in very low loadings films). However, this is no longer true if the dye is adsorbed as aggregates. For instance, the exciton theory[39,40] predicts a splitting in two excited states for dimers. The value and direction of their transition moments are given by the addition and the subtraction of the individual transition moment of the monomeric units; consequently, they depend on the geometry and orientation of the monomeric units in the dimer. In Scheme 1, different representative geometries for the dimer are analyzed:

(i) In a twisted sandwich-type dimer (both xanthene planes are parallely disposed) coplanar with the clay surface (case A in Scheme 1) the transition moments to both excited states of the aggregate will be orthogonally oriented in relation to each other and in the clay layer (*xy*-plane). In this case, and because there is not a preferential orientation in the layer plane (*x*- and *y*-directions are equivalents), neither of the two absorption bands of this dimer would present any anisotropy behavior. The same conclusion can be extended to a coplanar head-to-tail dimer (geometry not shown).

(ii) In an oblique head-to-tail dimer (case B, in Scheme 1), the addition of individual transition moments of the monomeric units (responsible for a bathochromic absorption band with respect to the monomeric one, the so-called J-band) will be oriented through the clay layer (*xy*-plane) and will not present any anisotropy. However, the subtraction of the individual transition moments will be oriented

(27) Hagerman, M. E.; Salamone, S. J.; Herbst, R. W.; Payeur, A. L. *Chem. Mater.* **2003**, *15*, 443−450.
(28) Chen, G.; Iyi, N.; Sasai, G.; Fujita, T.; Kitamura, K. *J. Mater. Res.* **2002**, *17*, 1035−1040.
(29) Iwasaki, M.; Kita, M.; Ito, K.; Kohno, A.; Fukunishi, K.; *Clays Clay Miner.* **2000**, *48*, 392−399.
(30) Umemura, Y.; Onodera, Y.; Yamagishi, A. *Thin Solid Films* **2003**, *426*, 216−220.
(31) Sasai, R.; Fujita, T.; Iyi, N.; Itoh, H.; Takagi, K. *Langmuir* **2002**, *18*, 6578−6583.
(32) Martínez, V.; López Arbeloa, F.; Bañuelos, J.; Arbeloa, T.; López Arbeloa, I. *Langmuir* **2004**, *20*, 5709−5717.
(33) Martínez, V.; López Arbeloa, F.; Bañuelos, J.; Arbeloa, T.; López Arbeloa, I. *J. Phys. Chem. B* **2004**, *108*, 20030−20037.
(34) Martínez, V.; López Arbeloa, F.; Bañuelos, J.; López Arbeloa, I. *J. Phys. Chem. B*, **2005**, *109*, 7443−7450.
(35) Lakowicz, J. R. *Principles of Fluorescence Spectroscopy*, 2nd ed.; Kluwer Academic: New York, 1999.
(36) Milch, J.; Thulstrup, E. W. *Spectroscopy with Polarized Light*; VCH Publishers: New York, 1986.
(37) Kliger, D. S.; Lewis, J. W.; Randall, C. E. *Polarized Light in Optics and Spectroscopy*; Academia Press: San Diego, 1990.
(38) Valeur, B. *Molecular Fluorescence. Principles and Applications*; Wiley-VCH: Weinheim, 2002.
(39) McRae, E. G.; Kasha, M. *Physical Process in Radiation Biology*; Academy Press: New York, 1964.
(40) Kasha, M.; Rawls, H. R.; El-Bayoumi, M. A. *Pure Appl. Chem.* **1965**, *11*, 371−392.

perpendicular to the clay layer (along the *z*-axis), and the corresponding absorption H-band (hypsochromically placed with respect to the monomeric one) will respond to the polarized light if the orientation angle between the incident light and the normal to the layer is changed. Indeed, an angle of 90° between the linearly polarized incident light along the *x*- or *y*-axes and the transition moment should be expected.

(iii) For coplanar displaced dimers (cases C in Scheme 1), the addition of the monomeric transition moments will be oriented along the long-molecular axis of the monomer units, and the system will present the same anisotropy effect as that for the monomer units. If the xanthene plane of the monomers lies more parallel to the clay layer, the displaced θ angle takes low values and the dimer would be characterized by a J-band ($\theta < 54.7°$, case C_2 in Scheme1), placed at longer wavelengths than the monomer absorption band. For a more perpendicular disposition of the monomer units with respect to the clay plane ($\theta > 54.7°$, case C_1 in Scheme1), the coplanar dimer will be characterized by a hypsochromic absorption H-band. So, the absorption spectroscopy with linear polarized light of R6G/Lap films can not only provide information about the orientation of the adsorbed molecules but can also discern the type of adsorbed aggregates in the films, since their response to the polarized light depends on the geometry of the aggregates.

Experimental Section

The sodium form of the synthetic laponite clay (Lap) was supplied by Laporte Industries, LPT. Lap clay is a smectite-type mineral with a general structural formulas $Na^{+}_{0.7}[(Si_8Mg_{5.3}Li_{0.7})O_{20}(OH)_4]^{0.7-}$ of the unit cell, with a cation exchange capacity (CEC) of 77.3 mequiv/100 g[41] and an adsorption area of 290 m^2/g[42] for the dried powdered sample, although the adsorption area can be theoretically increased up to 800 m^2/g for swollen sample in which all the interlayer space is available for adsorption.[43] Lap clay is also characterized by very high chemical purity, low iron content, and small particle size (<30 nm) providing transparent films in the Vis region and stable colloidal suspensions. Thin Lap films, supported on glass substrates, were obtained by the spin-coating technique (BLE spinner, model Delta 10) as described elsewhere.[32] Reproducible thickness of the films (around 250 nm in the center, as was previously estimated by Atomic Force Microscopy[32]) was obtained by controlling the viscosity of the clay suspension (20 g/L) and the rate of spinning (2500 rpm during 60 s). Films with 450 nm thickness were also used by repeating the spin-coating process twice.

Rhodamine 6G (R6G) was supplied by Kodak (laser grade) and was used as received. The intercalation of the dye into the film was carried out by ion exchange reaction, immersing the Lap films in a dye solution of water (Milli-Q)/ethanol mixture with a molar fraction in water of $x_w = 0.80$ at room temperature. The dye coverage on the Lap film was controlled by the concentration of the dye solution (10^{-5} and 10^{-3} M), the immersion time (from minutes to days), and the thickness of the film. After dye intercalation, the hybrid films were rinsed first with ethanol and later with pure water to abolish species in the external film surface. Finally, the films were dried overnight at 35° C and stored in darkness for several days to ensure an adequate distribution of the R6G molecules.[32] The final dye content into the Lap films, expressed by the percent of cation exchange capacity of the Lap (% CEC), was evaluated by elementary CHN analysis (Perkin-Elmer, model CHN 2400 analyzer) of the organic material in the films.

Scheme 2. Experimental Setup To Record Absorption Spectra with Linearly Polarized Light for Different Orientation of the Supported Films with Respect to the Incident Beam

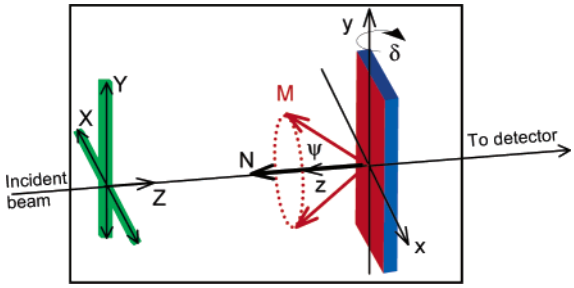

The X-ray diffraction (XRD) profiles of the films were recorded on a Philips PW-1710 diffractometer using Cu Kα radiation. XRD difractograms for pure Lap samples both in film and in powder were collected in the 2−60° interval with a scan speed of 1°/min, whereas the XRD profiles of R6G/Lap films were registered in the 2−20° range. Vis-absorption spectra of R6G/Lap films were recorded on a Varian spectrophotometer (model CARY 4E) in the 420−620 nm range by the transmittance method and 1 nm of bandwidth. Linearly polarized light was obtained by a birefringence prism-type Glan-Taylor polarizer (Harrick, reference PGT-S1V) characterized by a high efficiency in the UV−Vis region.[37] A depolarizer was placed after the sample in order to reduce the intrinsic polarization of the monochromator and other optical elements of the spectrophotometer.[44]

The anisotropy study was performed by recording the absorption spectra for horizontal (*X*-axis, A_X) and vertical (*Y*-axis, A_Y) polarized light with respect to the incident beam (*Z*-axis) for different orientations of the sample with respect to the incident light (for instance, by twisting the supported film around its *y*-axis at different δ angles), as is shown in Scheme 2. The dichroic ratio ($D_{X,Y}$), obtained from the relation between both spectra ($D_{X,Y} = A_X/A_Y$), was evaluated for δ angles from −70 up to 70°. The intrinsic responses of the optical components of the spectrophotometer were corrected by recording the dichroic response of the instrument of an isotropy sample, for instance a R6G solution 10^{-5} M in a 1 mm pathway cuvette, at every scanned δ angle.

Results and Discussion

Transparent supported films of Lap clay are obtained by the spin-coating technique. Besides, this technique provides a good distribution of the Lap particles in the supporting substrates, and the films are characterized by their low roughness and the absence of any cracks, as revealed by scanning electron and atomic force microscopies (SEM and AFM).[32] The macroscopic parallel orientation of the clay layers in the supported glass is corroborated by the X-ray diffraction technique. The XRD profile of a pure Lap film

(41) Van Ophen, H.; Fripiat, J. J. *Data Handbook for Clay Materials and Other Non-Metallic Minerals*; Pergamon Press: London, 1979.
(42) Fraile, J. M.; García, J. I.; Harmer, M. A.; Herrerías, C. I.; Mayoral, J. A.; Reiser, O.; Werner, H. *J. Mater. Chem.* **2002**, *12*, 3290−3295.
(43) Thompson, D. W.; Butterworth: J. T. *J. Colloid Interface Sci.* **1992**, *151*, 236−243.
(44) Thulstrup, E. W.; Milch, J. *Spectrochim. Acta* **1988**, *44A*, 767−782.

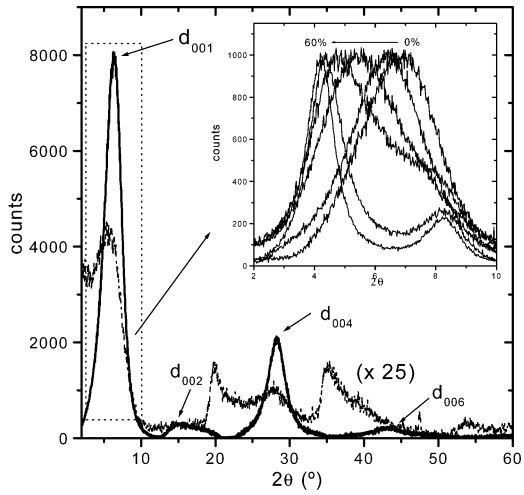

Figure 1. X-ray diffractions of Lap clay particles in supported film (solid curve) and in powder (dotted curve). The height-normalized profiles of R6G/Lap supported films for different dye loadings are also inset.

(Figure 1, solid curve) only reveals (00c) peaks, indicating a highly ordered stacking of the clay layers in the c-direction normal to the supporting surface. The (001) peak of the pure Lap films, centered at $2\theta = 6.9°$, indicates an interlayer distance of 12.8 Å, which after eliminating the thickness around 9.6 Å of a TOT clay layer leads to a clearance space of 3.2 Å. By comparison, the XRD pattern of a Lap powdered sample (Figure 1, doted curve) shows peaks placed in similar 2θ values but with an intensity ~50 times lower than that for the Lap film due to a semicrystaline lamellar structure of clay particles with a nearly random orientation of the clay particles in the powder sample.

The adsorption of R6G molecules in the interlayer space of Lap films is confirmed by XRD data. Included in Figure 1, the height-normalized XRD profiles of R6G/Lap films with dye content are shown. The 001 peak becomes sharper, more intense, and progressively shifts to lower 2θ values by increasing the dye loading, indicating a more ordered arrangement of the films in the *c*-axis and an increase in the basal interlayer space at high dye loadings.[27,45,46] A greater packing of the dye molecules in the interlayer space probably leads to a more perpendicular disposition of the adsorbed molecules and improves the stacking of the clay layers. Taking into account the molecular dimension of the R6G molecules (13.8 × 11.5 × 9.0 in Å, see **1**) obtained by the semiempirical AM1 quantum mechanic method, a perpendicular distribution of the long-molecular axis of R6G along the normal to the surface would lead to a covered adsorbed area of 103 Å^2 per adsorbed molecule. Because the area of Lap surface per charge unit is around 62 Å^2 (290 m^2.g^{-1}/0.773 × 10^{-3} equiv.g^{-1}), this means that for the R6G/Lap film with a loading of 60% CEC, the adsorption surface of Lap is saturated by dye molecules. Indeed, increasing the dye concentration of the immersion solution used for the intercalation process and/or the immersion time does not further increase the absorbance of the films, and consequently the amount of adsorbed dye becomes nearly constant from the 60% CEC loading.

Table 1 lists a progressive increase in the clearance space of Lap films with the dye loading, from 3.2 (0% CEC) up to 11.4 Å (60% CEC). This evolution can denote different orientations of the adsorbed molecules depending on the loading. If the interlayer space is given by the projection of the long-molecular axis of R6G (13.8 Å) to the *c*-axis, then the tilted ψ angle between the long-molecular axis and the normal to the surface can be estimated by means of cos ψ = interlayer space (in Å)/13.8 Å. The tilted angle evolves from 74° (very low loading films) to 33° (high loading films), as is also listed in Table 1. Therefore, R6G molecules are adsorbed more perpendicularly to the Lap surface as the dye content is increased, probably as a consequence of a high packing and compactness of the adsorbed molecules.

However, the XRD technique can only provide a rough estimation of the orientation ψ angle of the adsorbed molecules. Indeed, the obtained basal space is the average value for all the interlayer distances present in the films, but in low-moderate dye loadings not all the interlayer spaces are equally swelled.[47] Consequently, XRD data underestimate the ψ value. Moreover, interactions between dye molecules are not considered (e.g., aggregation phenomena) where different R6G species such as dimers, trimers, and/or high-order aggregates with different geometries and molecular sizes can be present. For this reason, UV−Vis absorption spectroscopy with linear polarized light is now applied to evaluate the orientation of R6G molecules adsorbed in Lap films.

Absorption spectra of R6G/Lap films with polarized light were recorded for five representative loadings: 0.1, 5.7, 22, 40, and 60% CEC, where different adsorbed R6G species were previously characterized.[33,34] For very diluted dye films (0.1% CEC) R6G molecules are adsorbed as monomeric units; dimers of R6G are characterized mainly in moderate loadings (1−25% CEC); and for high loadings (40−60% CEC), higher-order aggregates can be observed. The response of these species to the absorption of linear polarized light is now studied.

The absorption band of R6G monomers adsorbed on Lap films is centered at 528 nm. Figure 2 shows the evolution of this band for X- and Y-linear polarized light at different twisting δ angles, from 0 to 70° around the film *y*-axis, that is, the angle between the normal to the film and the *Z*-axis of the incident light (see Scheme 2). These spectra are corrected for the instrumental responses to the planes of the polarized light, for instance, by extrapolating the response of an isotropic system (an ethanolic solution of R6G at 10^{-5} M in a 1 mm pathway cell) to the X- and Y-polarized light for all the scanned δ angles. Since identical evolutions were observed by scanning the δ angle from 0 to −70°, only the changes in the absorption spectra from 0 to 70° are now discussed.

The response of the absorption band of R6G in Lap films to the X-polarized light (Figure 2A) by scanning the δ angle

(45) Bűjdak, J.; Iyi, N.; Fujita, T.; *J. Colloid Interface Sci.* **2003**, *262*, 282−289.
(46) Miyamoto, N.; Kawai, R.; Kuroda, K.; Ogawa, M. *Appl. Clay. Sci.* **2001**, *19*, 39−46.
(47) Endo, T.; Nakada, N.; Sato, T.; Shimada, M. *J. Phys. Chem. Solids* **1989**, *50*, 133−137.

Table 1. X-ray Diffraction Profile (peak position, 2θ, intensity, I, and full width at medium height, $\Delta\theta_{1/2}$) of R6G/Lap Films for Different Loadings (in % CEC). The 001 Interlayer Distance (d_{001}), the Free Interlayer Distance After Subtracting the TOT Layer Thickness (d_{free}), and the Tilted Angle Between the Long Molecular Axis of the Dye and the Normal to the Lap Layer (ψ, obtained from XRD and absorption with polarized light) are also included

	RX diffraction						polarized absorption	
% CEC	2θ (°)	I (counts)	$\Delta\theta_{1/2}$ (°)	d_{001} (Å)	d_{free} (Å)	ψ_{mean} (°)	$\psi_{<500}$ (°)	$\psi_{>500}$ (°)
0	6.9	1090	3.0	12.8	3.2			
0.1	6.6	1050	2.70	13.4	3.8	74	62	62
5.7	6.4	1580	2.85	13.8	4.2	72	48	61
14	5.5	1670	2.95[a]	16.1	6.5	62		
22	4.8	1710	2.68[a]	18.4	8.8	50	46	61
40	4.3/8.3[b]	3070	1.22	20.3	10.7	39	32	60
60	4.2/8.3[b]	4430	0.93	21.0	11.4	33	28	60

[a] Overlapping of two diffraction peaks ($d_{001} + d_{002}$). [b] Peaks corresponding to d_{002}.

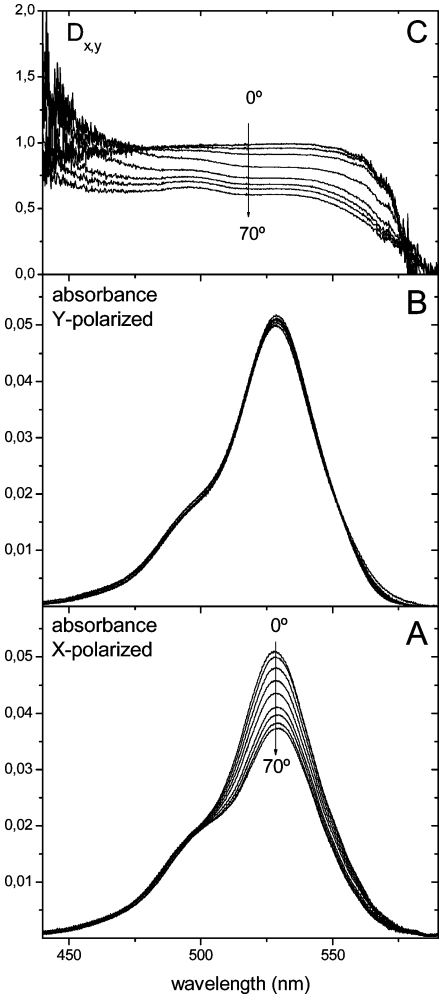

Figure 2. Evolution of the X- (A) and Y-polarized (B) corrected absorption spectra of the 0.1% CEC R6G/Lap film with different orientations of the film with respect to the incident beam. The corresponding dichroic ratios are also shown (C).

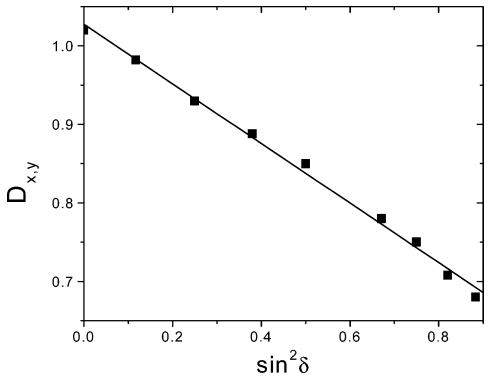

Figure 3. Linear relationship between the dichroic ratio obtained from the absorbance at 528 nm of the 0.1% CEC R6G/Lap film with the twisted δ angle of the sample. Similar lines are observed for other absorption wavelengths.

reveals a preferential orientation of the monomer units adsorbed in the Lap films toward the normal to the film (*z*-axis). The absence of any response to the Y-polarized light (Figure 2B) indicates an isotropic distribution of the transition moment of the monomers in the film layer (random distribution in both equivalent *x*- and *y*-directions); whereas the identical evolution of the X-polarized absorption spectra for positive and negative δ angles suggests that the vectorial addition of the transition moment of all adsorbed monomers results in a perpendicular orientation to the film plane, along the *z*-axis, indicating a regular orientation of adsorbed R6G molecules toward the *z*-axis and a random distribution in the clay film (*xy*-plane).

The dichroic ratio of the absorption spectra ($D_{X,Y} = A_X/A_Y$), obtained by the relation between the absorption spectrum with the vertical (*X*-axis) and the horizontal (*Y*-axis) polarized light, respectively, gradually decreases with the twisted δ angle (Figure 2C), and this evolution is constant for all the wavelengths of the absorption band. This is consistent with the presence of only one kind of R6G species for very low loading films, corroborating the adequate characterization of the R6G monomer in Lap films at this very low loading (0.1% CEC). As is shown in Figure 3, the $D_{X,Y}$ value linearly correlated against the $\sin^2\delta$ value, according to eq 1. From its slope, a tilted ψ angle of 62° between the transition moment (along the long-molecular axis of the aromatic ring of rhodamine dyes as predicted by quantum mechanic calculations) and the normal to the clay layers can be evaluated, independent of the analysis wavelength (Table 1).

For R6G/Lap films with loadings >1% CEC, the dye molecules self-associate. Dimers of R6G are characterized in the 1−25% CEC loading range.[33,34] The anisotropy of R6G dimers in Lap films is studied for two representative samples: 5.7 and 22% CEC. None of the recorded absorption spectra of R6G/Lap films can be considered as that of the pure R6G dimer, because the dimer is always in equilibrium with the monomers and/or high-order aggregates. In a preceding paper,[33] it was established that for moderate R6G/Lap loadings (1−25% CEC), R6G molecules only self-aggregate as dimer forms. The dimerization constant of R6G in Lap films was evaluated, from which the absorption spectrum of the dimer can be calculated by subtracting the

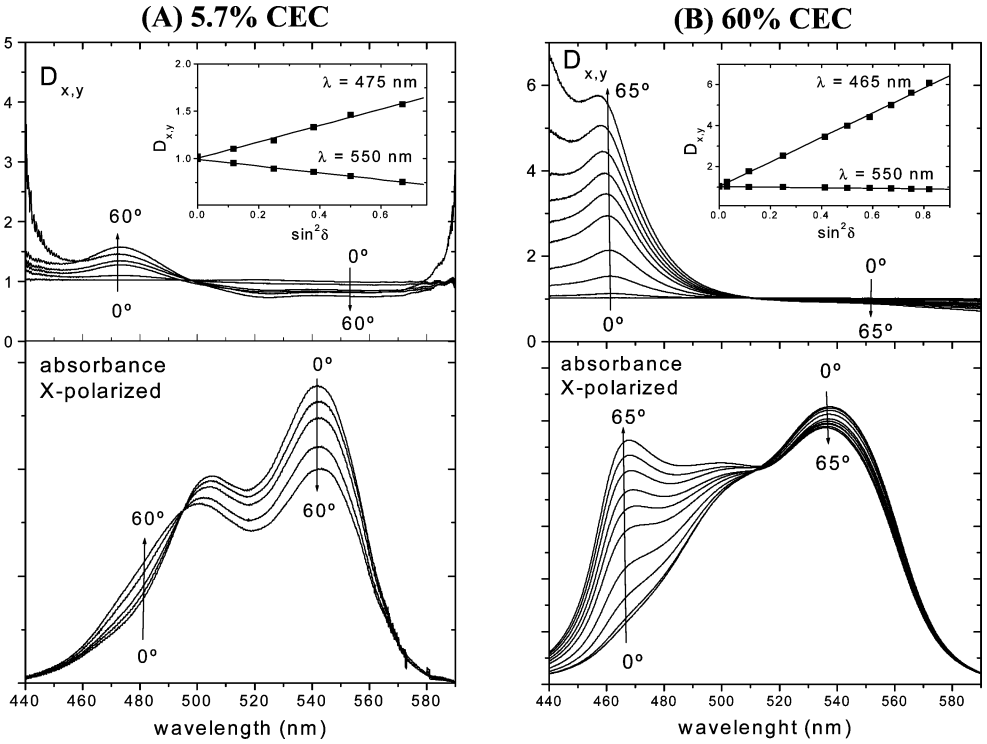

Figure 4. Corrected X-polarized absorption spectra (bottom) and dichroic ratio (top) of 5.7% (A) and 60% (B) CEC R6G/lap films for different orientations of the samples with respect to the incident beam. The linear relation between the dichroic ratio and the twisted δ angle at two representative short- and long-wavelengths are also inset.

proportion of the monomer absorption spectrum (that recorded at very low loadings, i.e., 0.1% CEC) from the experimentally recorded spectra at any loading in the 1−25% CEC. The absorption spectrum of the dimers presents two clear bands centered at 545 and 503 nm.[33]

Figure 4A shows the response of the absorption bands of the R6G dimer characterized in the 5.7% CEC film to the X-polarized light. The absorption spectrum of the dimer does not present any important change with the Y-polarized light (data non shown), suggesting an isotropic behavior of the adsorbed dimer in the Lap *xy*-plane, similar to the observation of the monomer absorption band (Figure 2B). However, the two absorption bands of the dimer present different anisotropic effects with respect to the vertically polarized light (Figure 4A, bottom): the absorption band placed at higher energies (H-band) increases with the twisted δ angle, whereas the opposite evolution is recorded in the lower energies band (J-band), leading to an isosbestic point at around 498 nm. This is better confirmed by the dichroic ratio (Figure 4B, top), where a positive and a negative evolution with the twisted δ angle are observed for the short- and the long-wavelength regions, respectively. At the isobestic point, the dichoric ratio no longer depends on the twisted angle. Present results indicate that the R6G dimers can adopt two different tilted angles with respect to the Lap layers (inset Figure 4A top): for the J-band a tilted ψ angle of 61° is obtained (similar to that observed for the monomer orientation in very low loading samples), whereas a more perpendicular orientation with a tilted ψ angle of around 48° is derived from the H-band

These tilted angles are not orthogonal to each other, and the present results with polarized light indicate that the two absorption bands of the dimers cannot be related with only one type of dimer with two absorption bands, but rather to two different types of dimers. Two different dimers were also previously claimed by both absorption and fluorescence spectroscopies with unpolarized light, although their nature was uncertain.[33,34] In the present paper, more precise information about the nature of both dimers can be derived. Since the transition moment of both dimers form a twisted ψ angle with respect to the normal to the clay layer, the xanthene plane of R6G units in the dimers cannot be parallelly or perpendicularly disposed with respect to the plane of the Lap films (cases A and C for $\theta = 90°$ in Scheme 1). Moreover, oblique head-to-tail dimers (case B in Scheme1) can also be excluded. Consequently, coplanar displaced dimers of R6G should be adsorbed in the Lap films. The absorption J-band should be ascribed to a coplanar dimer with a displaced angle $\theta < 54.7°$, which perfectly correlates with the twisted ψ angle (with respect to the normal to the clay layer) obtained for this absorption band of 61° (i.e., a tilted angle) $\theta = 90° - 61°$, of 29° with respect to the clay surface. This aggregate is named short-displaced coplanar dimer (case C (left) in Scheme1). On the other hand, the H-band should be assigned to the so-called long-displaced ($\theta < 54.7°$) coplanar dimer (case C (right) in Scheme1), although its dichroic ratio suggests a more parallel orientation, with respect to the Lap layer, of the monomeric units in the dimer, around $\theta = 90° - 48° = 42°$.

Similar qualitative values are observed for the two absorption bands of the dimers characterized for the 22% CEC R6G/Lap sample. The dimer identified by the J-band is inclined at the same angle ($\psi = 61°$, Table 1) as that observed in the 5.7% CEC sample, whereas the dimer

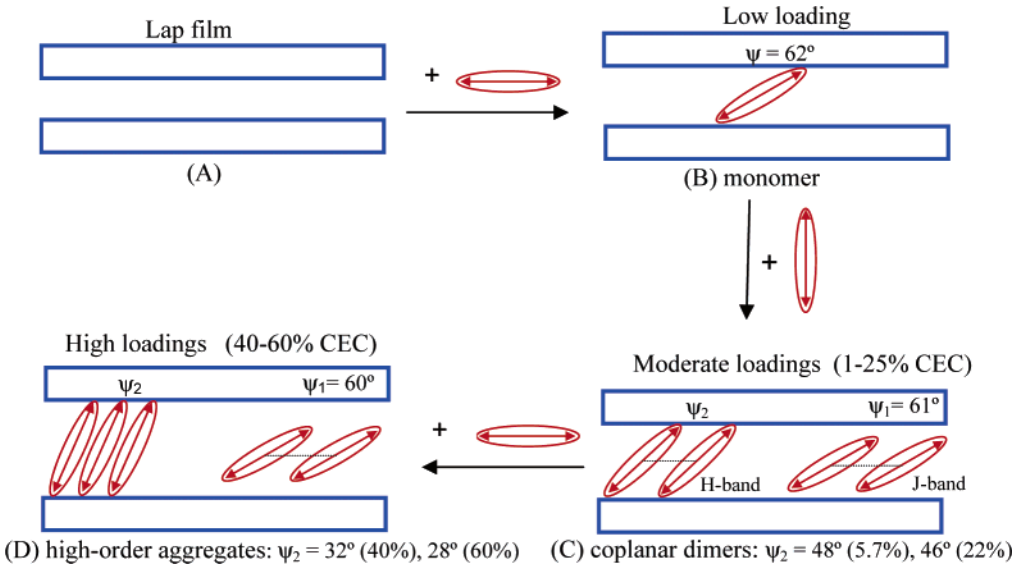

Figure 5. Schematic representation of the orientations and aggregations of R6G molecules adsorbed in Lap films for different loadings.

associated with the H-band adopts a more perpendicular distribution ($\psi = 46°$, Table 1) than that observed for the 5.7% CEC sample.

Finally, an identical procedure is applied to R6G/Lap films with very high dye loadings (>40% CEC), where higher-order aggregates of R6G were identified by an absorption band placed at around 468 nm.[33] Figure 4B (bottom) shows the anisotropic response of the absorption spectrum to the X-polarized light for the dye-saturated 60% CEC film. This absorption spectrum does not present any response to the Y-polarized light, suggesting again the isotropic behavior in the clay plane. The intensity at around 465 nm considerably increases with the twisted δ angle, indicating a near perpendicular distribution of the higher-order aggregates with respect to the Lap surface. Indeed, the dichroic ratio (Figure 4B, top) reveals two different spectral regions: that below 500 nm, with an important increase in the dichroic ratio with the δ angle; and a second range (above 500 nm) with a slight diminution in the dichroism with the δ angle. According to eq 1, the linear relationship between the dichroic ratio $D_{X,Y}$ and the $\sin^2 \delta$ value (inset Figure 4B, top) provides two different orientations of the adsorbed dye molecules: an orientation ψ angle of 60° for the transition moment responsible for absorption band placed at longer wavelengths (>500 nm), similar to that observed for other loadings at this spectral region; and a more perpendicular inclination ψ angle of 28° with respect to the film normal for the short-wavelengths absorption region (<500 nm) (Table 1).

Similar qualitative results are obtained for the 40% CEC sample. The ψ angle for the lower energetic part of the absorption spectrum ($\gamma_{>500} = 60°$, Table 1) is very similar to that observed for the 60% CEC sample and quite similar to that observed for all the other samples. The tilted ψ angle for the higher-order aggregates with an absorption band at around 465 nm for the 40% CEC film, with a ψ value around 32° (Table 1), is not so perpendicular to the Lap layer as that for the 60% CEC ($\psi = 28°$), although it is not so parallel as that observed for the dimers in moderate loadings (5.7 and 22% CEC, $\psi \approx 47°$). These results indicate that the aggregate responsible for the absorption H-band adopts a more perpendicular orientation with respect to the Lap layers as the dye content in the films is increased.

Consequently, present results on the orientation of R6G molecules adsorbed in Lap films with polarized light indicate that the R6G molecules can be oriented with two preferential angles with respect to the normal of the surface (Figure 5). A first orientation, where the xanthene plane is disposed nearly parallel to the clay layer with a tilted angle $\theta = 90° - \psi$ around 29°, is present in all samples, independent of the dye content. Because this orientation is adopted by R6G molecules in very diluted films and it should probably correspond to that in which the dye−clay interaction is optimized. Such an arrangement of the monomer units helps the formation of long-displaced coplanar aggregates with a displaced angle $\theta < 54.7°$, responsible for the observed bathochromic J-band in the absorption spectrum (case C in Scheme1).

As the dye content is increased, R6G molecules are packed more and more perpendicularly to the Lap surfaces (Figure 5). With this orientation, the formation of short-displaced coplanar aggregates with $\theta > 54.7°$ are favored. Consequently, a hypsochromic H-band is observed in the absorption spectra. This disposition of the adsorbed molecules is probably adopted to reduce the area per adsorbed monomer units to enhance the compactness and stacking of the dye molecules in high loading samples. Therefore, the increment in the interlayer space with the dye content is due to the formation of short-displaced coplanar (H-type) aggregates, which act as pillars to accommodate other more horizontal orientations in the clay layers of the adsorbed dye molecules.

A more perpendicular orientation in high loading samples of guest molecules in layered systems is a general tendency observed for several aromatic compounds embedded in different lamellar matrixes, such as other clays,[25−28] layered metal-halides,[48] monolayer systems,[49] and polymer-clay

(48) Era, M.; Miyake, K.; Yoshida, Y.; Yase, K. *Thin Solid Films* **2001**, *393*, 24−27.
(49) Kajikawa, K.; Yoshida, I.; Seki, K.; Ouchi, Y. *Chem. Phys. Lett.* **1999**, *308*, 310−316.

composites.[26,50] Moreover, a similar tilted $\theta = 90° - 25° = 65°$ angle is proposed in the saturated samples for most cases. Probably, this inclination angle is a consequence of guest−guest interactions; for instance, that responsible for the molecular aggregation. Such an inclination promotes coplanar aggregates with a displaced angle around 65°. For this angle, the inter-electronic π-system interactions of the chromophore units in the aggregates could be favored, for instance, presenting a minimum in the potential energy curve for a displaced angle. Indeed, crystallographic data for the aggregation of pyrene molecules to form the excimer in the crystalline state provide experimental evidences for a displaced coplanar aggregate.[51]

Conclusions

R6G molecules are adsorbed in the interlayer space of Lap films by cation exchange mechanism. The X-ray diffraction technique suggests that the interlayer space of Lap films increases with the dye loading, because the adsorbed dyes adopt a more perpendicular disposition with respect to the clay surface as the dye content is increased. Absorption spectroscopy with linearly polarized light reveals the anisotropy behavior of dye molecules adsorbed in supported films of clays as a consequence of a preferential orientation of the dye with respect to the clay layers. Adsorbed R6G molecules can adopt two preferential orientations with respect to the normal to the film: a near parallel disposition of the monomer units (with an inclined angle around 28° with respect to the clay plane) leads to long-displaced coplanar aggregates characterized by a J-absorption band observed in all the loading range; the R6G molecules also adopt a more perpendicular orientation with respect to the Lap layers in high loadings. As the dye content is increased, the dye molecules tend to assume a more perpendicular orientation in order to increase the compactness of the adsorbed dyes and reduce the area per adsorbed molecule. This arrangement reduces the displacement of coplanar aggregates, and H-bands are observed in the absorption spectra.

Acknowledgment. This work is supported by the Spanish MEC Minister (Research Project MAT2004-04643-C03-02). V.M.M thanks the MECyD Minister for a research grant.

Supporting Information Available: An appendix showing the mathematical procedure. This material is available free of charge via the Internet at http://pubs.acs.org.

CM050728K

(50) Kim, D. W.; Blumstein, A.; Kumar, J.; Tripathy, S. K. *Chem. Mater.* **2001**, *13*, 243−246.
(51) Birks, J. B. *Photophysics of Aromatic Molecules*; Wiley Interscience: London, 1970.